Applied Scientific Research 44: 27–42 (1987)

A model of a casting

S.C. FLOOD * & J.D. HUNT
Dept. of Metallurgy and Science of Materials, University of Oxford, Parks Road, Oxford OX1 3PH, UK; (present address: Alcan International Ltd., Banbury Laboratories, Southam Road, Banbury, Oxon OX16 7SP, UK)*

Abstract. A model of a casting is presented which describes the freezing of a mushy zone, growing with a dynamically calculated undercooling at the dendrite tips. Equiaxed grains are introduced ahead of a columnar front. The model resembles a combination of the Stefan and mushy zone problems.

Nomenclature

Symbol	Meaning
c_0	composition
C	heat capacity per unit volume
C_1, C_2, C_3	parameters
D	solutal diffusion coefficient
g	weight fraction
G	temperature gradient
h	heat transfer coefficient
H	heat content or enthalpy per unit volume
I	nucleation rate per unit volume
k	distribution coefficient
k_i	thermal conductivity ($i = s$ or l)
K_i	thermal conductivity of a single phase ($i = s$ or l)
L	latent heat per unit volume evolved at the front
m	liquidus slope
N	number of grain per unit volume
N^0	number of substrate particles per unit volume
r	extended radius of a grain
t	time
T	temperature at time t
v	velocity
x	distance
α	width of control volume immediately ahead of the columnar front
β	width of control volume immediately behind the columnar front
δ	boundary layer thickness
δt	time discretisation interval
δx	spatial discretisation interval
ΔH	latent heat per unit volume
ΔT	undercooling
χ	pseudo heat transfer coefficient
ω	extended volume fraction of grains
Ω	volume fraction of grains

Subscript	Meaning
e	east face of the control volume
E	centre of the control volume to the east
ex	of the mould
L	liquidus
l	liquid
0	Centre of the control volume
s	solid
w	west face of the control volume
W	centre of the control volume to the west

Superscript	Meaning
B	bulk
I	columnar front
m	modified
p	pure
*	equiaxed
'	at time $t + \delta t$
$-$	average

1. Introduction

Solidification involves heat and fluid flow and, for an alloy, the transport of solute as well. The modelling of castings has concentrated on heat flow and has tended to introduce solute and fluid flow by simple, empirical treatments, if at all.

Two classes of heat flow models can be identified:

1. Stefan-type models, in which the latent heat is liberated discontinuously at a sharp phase front and where, therefore, a Stefan 'jump' boundary condition (see equation (5)) must be applied [1,2]; and
2. Mushy zone models, in which the latent heat is evolved continuously over a temperature range [3,4] and a Stefan 'jump' condition is not involved because there is not a discontinuity in solid fraction across the casting.

The former are good representations of the solidification of a pure metal, while the latter are used to describe alloy solidification.

Macroscopic solidification models have tended to neglect the undercooling at the phase front. Recently, however, Flood and Hunt [5,6] have produced a model which combines the characteristics of the Stefan and mushy zone models and which is capable of calculating a variation in undercooling of a semi-solid front. A Stefan 'jump' boundary condition is applied in the vicinity of the dendrite tips and the semi-solid is treated as in a mushy zone model. The undercooling at the columnar front varies as a result of the heat flow and generation in the casting and equiaxed grains can exist in the bulk. Clyne has

previously introduced a constant undercooling at a semi-solid front [7] and also has modelled a planar front with a varying undercooling [8] but the work described here is the first to include a varying undercooling at a semi-solid front and equiaxed grains ahead of it.

2. The model

The authors wanted to investigate, through the application of a mathematical model, whether the columnar-equiaxed transition can be explained in terms of the growth of equiaxed grains in the bulk and their thermal interaction with the columnar front. This required a model which included a dynamically calculated undercooling at the columnar dendrite tips because this undercooling is crucial in determining the velocity of the columnar dendrites and the growth rate of the equiaxed grains.

The key to the model is the relationship linking the velocity of a dendrite tip to its undercooling (this is applied to both the columnar and equiaxed dendrites):

$$v = \frac{C_1}{c_0}(\Delta T)^2 \tag{1}$$

where C_1 is a function of material constants [9]. The relationship is supported by both experimental measurements and an approximate analytical treatment of solute diffusion at the dendrite tip [9,10]. Modifications can be introduced with high temperature gradients, and other, more suitable growth velocity undercooling expressions can be used similarly to achieve closure under rapid solidification conditions [8].

The Scheil equation is used to describe the shape of the dendrites in the columnar semi-solid (this is a common technique, see references [11,7,12,5]) and the liquid volume fraction within an equiaxed grain. It is a function of temperature alone if a linear liquidus is assumed:

$$g_l = \left(\frac{T - T_L^P}{T_L - T_L^P} \right)^{1/(k-1)} \tag{2}$$

The assumptions behind the Scheil equation are discussed elsewhere [12]. The equation can be modified to account for solid state diffusion of solute (this is often important for interstitial solute, e.g. carbon in iron) and forward diffusion of solute down the interdendrite composition gradient [13,14].

The columnar dendrites are truncated Scheil shapes (see Fig. 1). The temperature at which the truncation occurs is calculated by iterating on the Stefan 'jump' condition (see later). The truncated Scheil and true dendrite shapes will deviate near the tips but will match within a short distance behind them. The discrepancy between the real and truncated Scheil shapes is not important because it occurs over only a small distance compared to the scale of the casting and because the correct quantity of latent heat is liberated after a very small distance behind the dendrite tips.

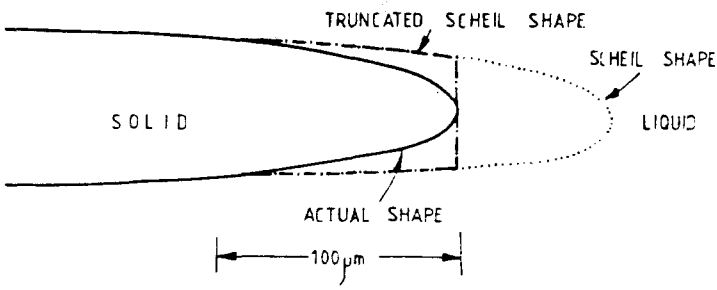

Fig. 1. The relationship between the complete Scheil, truncated Scheil and actual dendrite shapes.

The thermal fields of neighbouring grains are assumed to overlap because of the high thermal diffusivity of metals, and so the grains are isothermal and grow at the local bulk undercooling. A treatment has been developed to allow for a temperature difference between the grains and the bulk, but this is found to be negligible [6].

Impingement of the grains is accounted for by an Avrami-type treatment [15]: the concept of 'extended' volume, ω, as opposed to the actual volume, Ω, enables the kinetics of the growth of the equiaxed grains to be divorced from the geometrical complication of impingement. The increase in the actual volume fraction of grains, $d\Omega$, is related to the change in the 'extended' volume fraction, $d\omega$, by

$$d\Omega = (1 - \Omega)\, d\omega$$

Fluid flow is assumed not to affect heat flow in the semi-solid because of the high thermal diffusivity of metals and the small interdendritic spacings. In the bulk, convection is modelled by a temperature plateau ahead of a conducting boundary layer and quantities are described by bulk values. A small boundary layer corresponds to much convection in the bulk. In a recent version of the model, the size of the boundary layer is a function of the volume fraction equiaxed in the bulk.

In the first instance, nucleation of the grains was ignored. The influence of just the growth of the grains on the columnar-equiaxed transition was considered; grains were assumed always to be present in the bulk and they started to grow as soon as the local temperature fell below the liquidus. Later, calculations were performed with a temperature dependent nucleation rate [16,6]. Assuming heterogeneous nucleation in which substrate particles are consumed by the growing equiaxed grains, and that each substrate only nucleates one grain, the nucleation rate is given by:

$$I = N^0 \frac{(N^0 - N)}{N^0} (1 - \Omega) C_2 \exp\left(-C_3/(\Delta T^*)^2\right)$$

and typical values for C_2 and C_3 are 10^{29} s^{-1} m^{-3} and $46K^2$ respectively.

On the basis of an argument which considers the probability of a columnar dendrite being obstructed by an equiaxed grain in the bulk, the columnar-

equiaxed transition is assumed to occur when $\Omega = 0.49$ immediately ahead of the front [6,17].

3. Mathematical formulation

The model can be applied to one, two or three dimensions. As an example, consider the one dimensional case (see Fig. 2). Solidification is modelled by modifying the Fourier heat conduction equation:

$$C^m\left(\frac{\partial T}{\partial t}\right) = \frac{\partial}{\partial x}\left(k_i\left(\frac{\partial T}{\partial x}\right)\right) + (1 - g_l)\frac{\partial \Omega}{\partial t}\Delta H \tag{3a}$$

where C^m is the modified heat capacity:

$$C^m = C + \Omega \Delta H \frac{\mathrm{d}g_l}{\mathrm{d}T} \tag{4}$$

with g_l defined by the Scheil equation (2). $\Omega = 1$ in the columnar semi-solid and is the local volume fraction of equiaxed crystals in the bulk. $\partial\Omega/\partial t = 0$ in the columnar zone. ΔH is the total latent heat per unit volume of liquid.

In a simple treatment of convection in the bulk, the diffusive term in (3a) is replaced by one involving a pseudo-heat transfer coefficient, χ, which is a function of the boundary layer width, δ:

$$C^m\left(\frac{\partial T}{\partial t}\right) = \chi\left(T_l^B - T^I\right) + (1 - g_l)\frac{\partial \Omega}{\partial t}\Delta H \tag{3b}$$

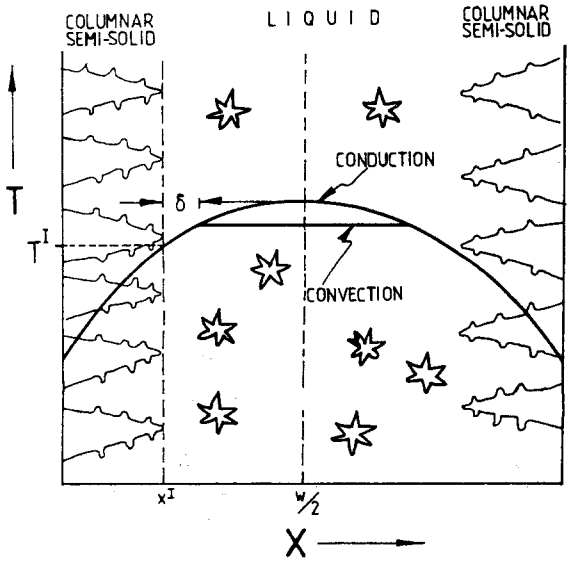

Fig. 2. The model system with and without convection in the bulk.

where T^I is the temperature of the columnar front and

$$\chi = \frac{k_l}{\delta}$$

The value to be used for δ is uncertain. The authors have used values ranging from 200 microns to the width of the casting; the true value must lie somewhere in this range. In more thorough treatments of convection, the heat transport is modelled within the boundary layer as well [6].

The boundary conditions are:

$$\frac{\partial T}{\partial x} = h(T - T_{ex}) \text{ at the edge}$$

where h is the heat transfer coefficient representing the resistance between the casting and the mould wall and T_{ex} is the mould temperature;

$$k_i \frac{\partial T}{\partial x} = 0 \text{ at the centre of the casting}$$

and the Stefan 'jump' condition:

$$\left.\begin{aligned} vL &= k_s^I G_s^I - k_l^I G_l^I && \text{with conduction in the bulk} \\ vL &= k_s^I G_s^I - \chi\left(T_l^B - T_l^I\right) && \text{with convection in the bulk} \end{aligned}\right\} \tag{5}$$

is applied at the columnar front, with v given by (1) and L by

$$L = \left(1 - g_l^I\right)\Delta H. \tag{6}$$

In the bulk:

$$\frac{\partial \Omega}{\partial t} = (1 - \Omega) N 4\pi \bar{r}^2 v^* = (1 - \Omega) N 4\pi \bar{r}^2 \frac{C_1}{c_0} (\Delta T^*)^2$$

where N is the number of grains per unit volume, $\bar{r}$ is the local average extended grain radius and ΔT^* is the local undercooling.

The thermal conductivity varies as:

$$k_i = K_l + (1 - g_l)(K_s - K_l).$$

See reference [6] for further details.

4. Computational procedure

A fully conservative (or strong) discretisation of the governing differential equation (3) is adopted; the conservative property of the scheme proved very useful when debugging the computer code.

In the one-dimensional case, a representative cross-section of the casting is split into a row of control volumes. The change of temperature over time at the centre of a box is calculated by an explicit finite difference scheme. Discretisation equations are used to step through time in small intervals δt; the box temperature at time $t + \delta t$ are obtained explicitly from those at time t.

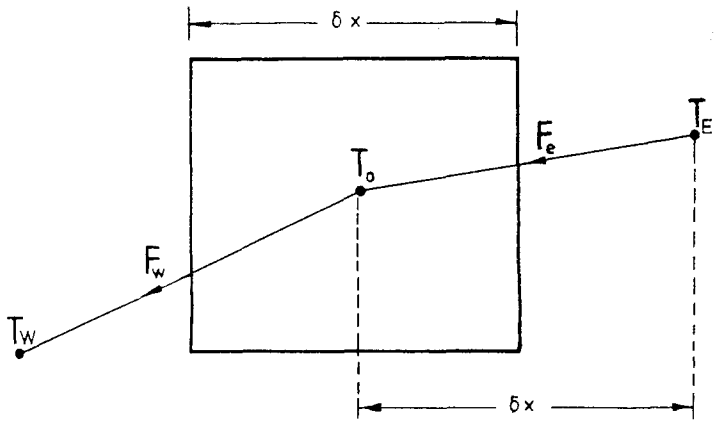

Fig. 3. A typical control volume.

The temperature dependency of the thermal conductivity is easily handled by employing the values for conductivity at the box faces. As examples of the form of the discretisation equations, consider respectively those for heat transport in the columnar semi-solid (see Fig. 3):

$$T_0' = T_0 + \frac{\delta t}{C_s^m (\delta x)^2}\left(k_w T_W - (k_w + k_e)T_0 + k_e T_E\right)$$

and the bulk liquid, with conduction:

$$T_0' = T_0 + \frac{\delta t}{C_s^m}\left[\frac{(k_w T_W - (k_w + k_e)T_0 + k_e T_E)}{(\delta x)^2} + (1 - g_l)\Delta H \delta \Omega_0\right]$$

where C_s^m is given by equation (4) and:

$$\delta\Omega_0 = (1 - \Omega_0) N 4\pi r_0^2 v_0^* \delta t.$$

The columnar front is tracked directly. It begins to move inwards once the temperature at the edge falls below some predetermined value at which nucleation occurs. From then on, at the start of each time interval, the 'jump' condition at the columnar front is invoked iteratively to determine the temperature and velocity of the front. The distance moved by the front in an interval δt is $v \cdot \delta t$. The columnar front constitutes the common face of the last semi-solid and the first liquid boxes (see Fig. 4). In the early numerical schemes, the dimensions of these two boxes change as the front advances. To ensure numerical stability (for a given δt there is a minimum permitted control volume dimension [18]) and accuracy, it is necessary to amalgamate and divide respectively the boxes immediately ahead and behind the front. Smoother solutions are obtained in the later schemes by repeatedly shrinking and joining liquid boxes at the centre of the casting instead of immediately ahead of the front [6].

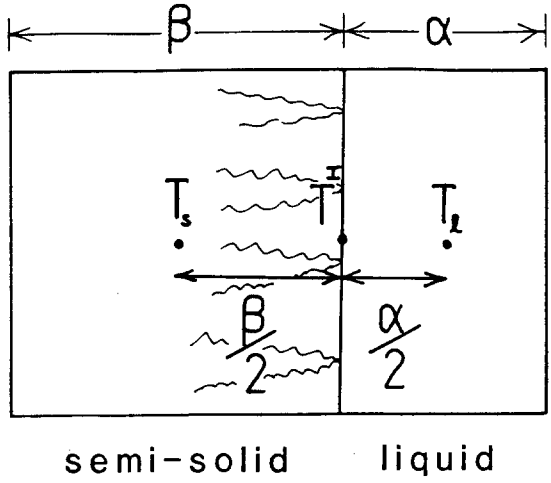

Fig. 4. The control volumes either side of the columnar front.

An explicit method is employed because the position of the front and its temperature are not known *a priori* at any stage in the calculation. An implicit scheme requires iterations at each time step to determine a consistent front position, temperature and velocity. It was thought that this would be very time-consuming but experience with the explicit iterative procedure used to satisfy the 'jump' condition suggests that convergence would be rapid. Consequently an implicit predictor-corrector implementation of the model is being developed, in which, additionally, a mapping is also used to immobilise the columnar front in computational space, hence avoiding the need for amalgamation and division of boxes.

Calculations have been performed in two dimensions with cylindrical control volumes and, in principle, can be extended to the third dimension.

5. Implementing the 'jump' condition

The truncation of the columnar dendrites at an undercooling causes a discontinuity in the latent heat liberation and requires the application of the Stefan 'jump' condition there. This boundary condition cannot be absorbed into the formulation by expressing the problem in the usual integral, control volume enthalpy approach [2,3] because the undercooling of the dendrite tips is not fixed *a priori* and equiaxed solid exists ahead of the front; it is impossible to define the enthalpy function in advance. The front has to be tracked directly and the parabolic velocity relation (1) provides the necessary closure for the temperature.

At the start of a time interval, the temperatures at the centres of the boxes either side of the columnar front, T_s and T_l, are known from the calculation of the previous time step. But the consistent value for T^I for the new time step

has yet to be determined. The gradients at the front can be approximated by (see Fig. 4):

$$G_s = 2k_s^I \frac{(T^I - T_s)}{\beta}$$

$$G_l = 2k_l^I \frac{(T_l - T^I)}{\alpha}$$

If E_j is the error in T^I at the j^{th} iteration then a value for T^I consistent with the 'jump' condition (5) can be obtained by iterating and finding progressively better values for T^I, according to the scheme:

$$E_j := \frac{(vL - k_s G_s^I + k_l G_l^I)}{pG_s^I - qG_l^I - \gamma_1 k_l^I + \gamma_s k_s^I - bL - \lambda v}$$

$$T_{j+1}^I := T_j^I + E_j$$

$$j := j + 1$$

until E_j is acceptably small. The symbols used in the expression for E_j are defined to be:

$$p = \frac{\mathrm{d}k_s^I}{\mathrm{d}T^I} \quad q = \frac{\mathrm{d}k_l^I}{\mathrm{d}T^I} \quad \gamma_1 = \frac{\mathrm{d}G_l^I}{\mathrm{d}T^I} \quad \gamma_s = \frac{\mathrm{d}G_s^I}{\mathrm{d}T^I} \quad b = \frac{\mathrm{d}v}{\mathrm{d}T^I} \quad \lambda = \frac{\mathrm{d}L}{\mathrm{d}T^I}.$$

Having found T^I, the velocity and latent heat at the front can be calculated using equations (1) and (6).

6. Results

Calculations were performed using physical parameters relating to Al–Cu alloys ($T_L^p = 933\text{K}$; $m = -2.6K$ wt%$^{-1}$; $k = 0.18$; $C = 3400$ kJ K^{-1} m^{-3}; $\Delta H = 1.02 \times 10^9$ J m^{-3}; $K_s = 180$ W m^{-1} K^{-1}; $K_l = 98$ W m^{-1} K^{-1}; $C_1 = 3 \times 10^{-4}$ ms^{-1} K^{-2} wt%$^{-1}$). Values of heat transfer coefficient were chosen to produce freezing times comparable to sand and metal mould castings, and some calculations with rapid solidification conditions have also been undertaken and are discussed briefly later. Unlike previous mushy zone models, the dynamically calculated undercooling at the front enables the model to produce cooling curves which exhibit recalescence. Most have been for one-dimensional castings (slit moulds) (see Fig. 5). The cooling curves show a higher bulk temperature during solidification when equiaxed grains are present owing to the liberation of latent heat ahead of the front. Also the columnar curves show a slight recalescence throughout freezing because of a deceleration of the front due to the increasing liberation of latent heat behind it as the semi-solid region increases. This last observation is peculiar to one-dimensional slit castings; in a cylindrical casting, the area of the columnar front decreases as it nears the centre of the casting and this causes a decreasing

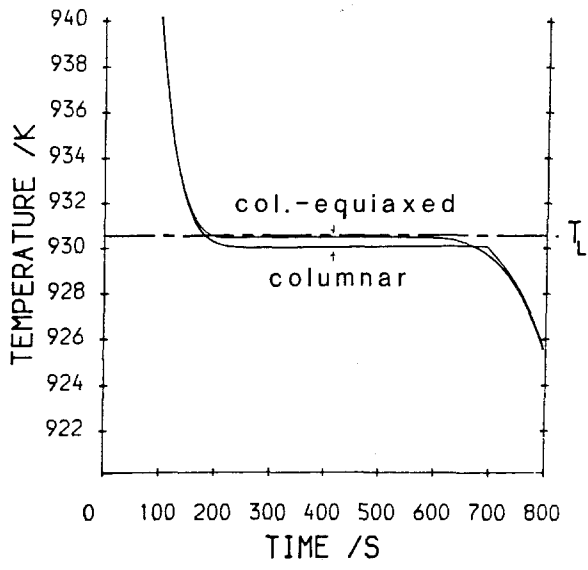

Fig. 5(a).

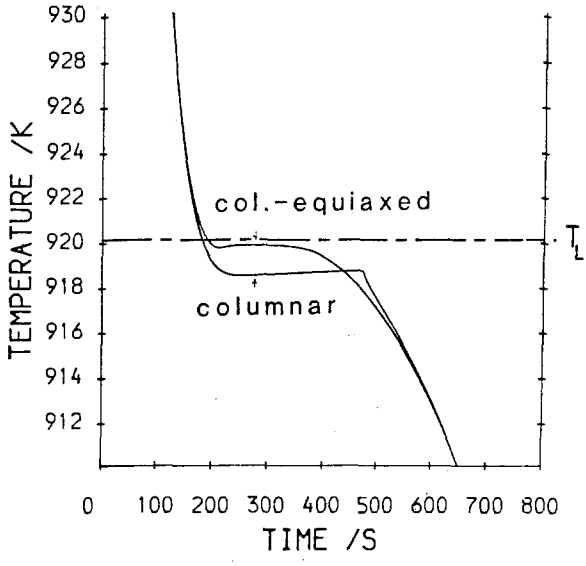

Fig. 5(b). Cooling curves for Al–Cu alloys with and without equiaxed grains ahead of the columnar front: (a) Al-1 wt% Cu (no convection); (b) Al-5 wt% Cu (no convection); and (c) Al-5 wt% Cu (convection in the bulk; $\delta = 0.2$ mm) (see p. 37). All cast at 973 K into a 100 mm wide slit mould. $h = 10^2$ Wm^{-2} K^{-1}.

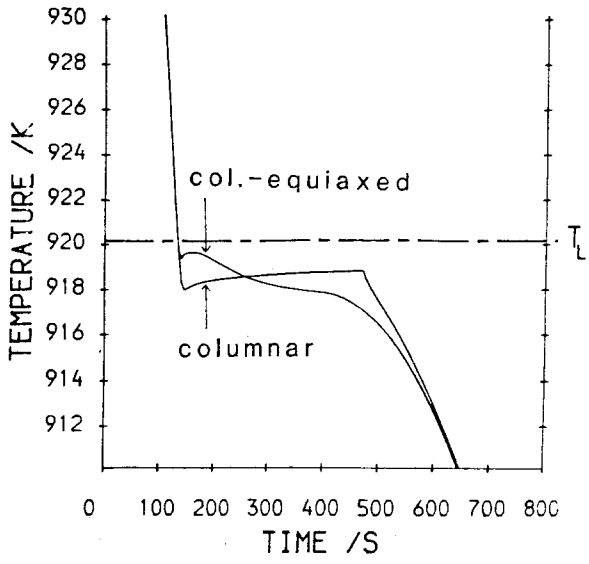

Fig. 5(c). See p. 36 for caption.

rate of latent heat production and, therefore, a drop in temperature (see Fig. 6).

Compare Figs. 5(a), (b) and (c). For a given rate of heat extraction, increasing the composition of an alloy causes an increase in the velocity and

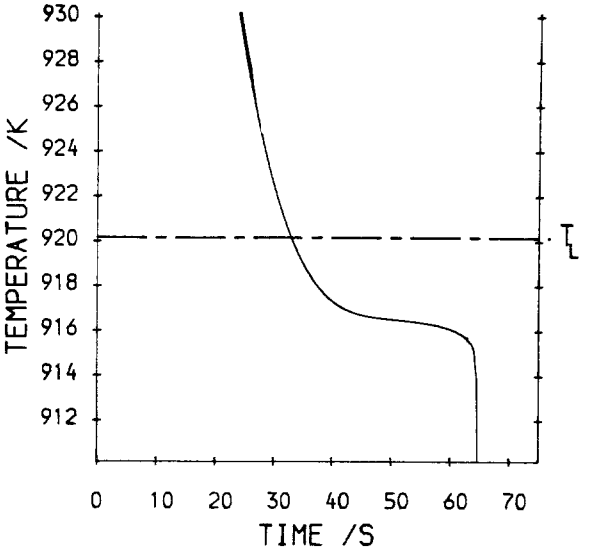

Fig. 6. Cooling curves for the columnar solidification of Al-5 wt% Cu alloy in a 100 mm diameter cylindrical mould. Poured at 973 K; $h = 10^3$ Wm^{-2} K^{-1}. No convection.

undercooling of the columnar front, and the temperature plateau in the cooling curve becomes shorter and further below the equilibrium liquidus temperature. This trend is a consequence of

(i) the compositional dependency of the velocity-undercooling relation (1) and
(ii) the variation in the Scheil solid fraction with composition.

Initially, the development of the equiaxed zone was investigated by placing nuclei ahead of the columnar front and allowing them to grow as soon as the local temperature fell below the liquidus. The scale and speed of equiaxed growth ahead of the columnar front depended only on the extent and degree of the undercooled liquid in the bulk:

(i) Increasing the composition promoted equiaxed growth by increasing the undercooling at the front (see Fig. 7).
(ii) Both decreasing the superheat and
(iii) decreasing the rate of heat extraction produced a lower temperature gradient in the bulk, thereby widening the undercooled layer and increasing the period in which the equiaxed grains could grow before the front reached them (see Figs. 7(a) and (b)).
(iv) Convection in the bulk accelerated the loss of the superheat and the onset of undercooling at the centre of the casting and therefore encouraged the growth of the equiaxed grains (see Fig. 7(c)).

In the calculations, when only the growth of the grains is considered, very small columnar ranges are produced. At moderate cooling rates, low tempera-

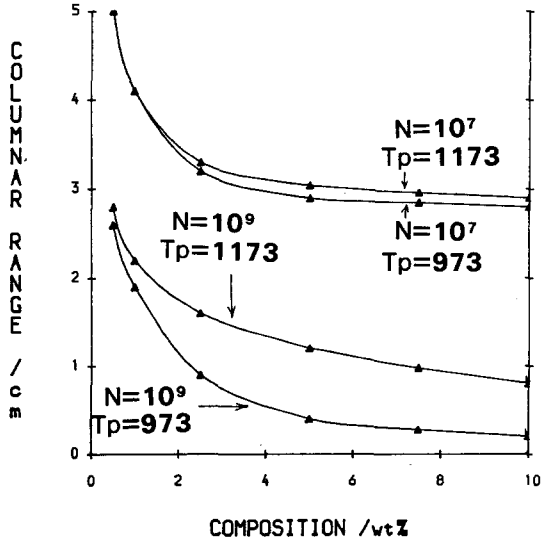

Fig. 7(a).

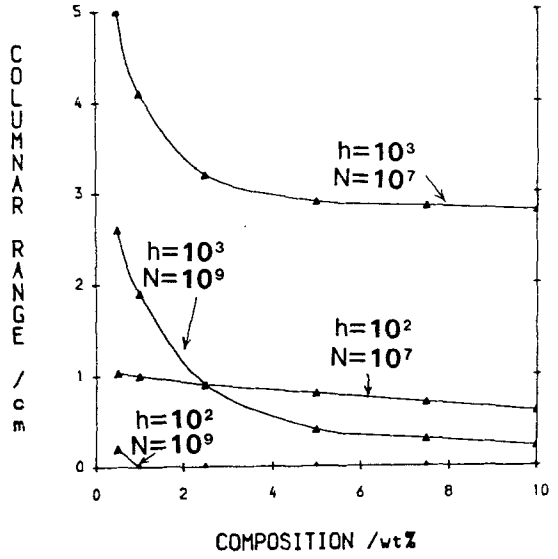

Fig. 7(b).

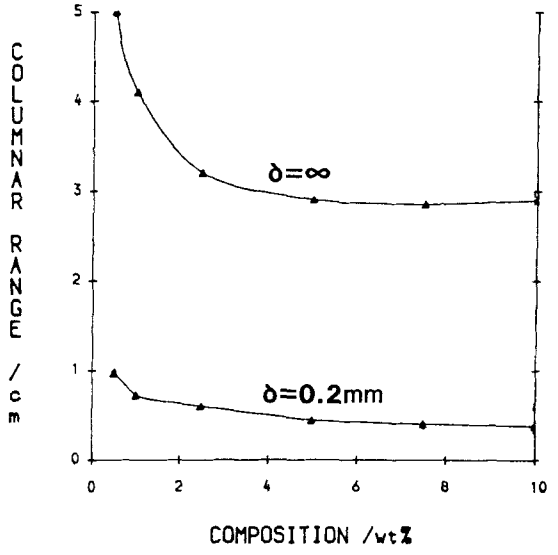

Fig. 7(c). Graphs of columnar range vs composition for Al–Cu alloys cast in a 100 mm wide slit mould. (a) The effect of grain density (N in m^{-3}) and pouring temperature (T_p in K). $h = 10^3$ Wm^{-2} K^{-1}; 10^9 grains m^{-3}. No convection. (b) The effect of heat transfer coefficient (h in Wm^{-2} K^{-1}) and grain density (N in m^{-3}). Poured at 973 K. No convection. (c) The effect of convection (δ = boundary layer width). Poured at 973 K; $h = 10^3$ Wm^{-2} K^{-1}; 10 grains m^{-3}.

ture gradients are quickly attained throughout the bulk and equiaxed growth soon occurs at the centre; even with high cooling rates which produce steeper gradients, growth immediately ahead of the front is fast. The difference

between the undercooling and, therefore, the tip velocities, of the columnar and equiaxed dendrites is not very great and so obstruction of the front occurs readily.

In practice, the equiaxed growth appears not to be so dominant. Hence, in reality, factors other than the growth of the equiaxed grains must also determine macrostructure, such as the buoyancy of the grains and their convective motion in the liquid. These effects would tend to reduce the presence of equiaxed grains ahead of the columnar front. The buoyancy of the grains is being investigated currently.

As expected, the model shows that the superheat is quickly removed owing to the low Stefan number and high thermal conductivity of metals – the rate-determining process during solidification is the removal of the latent as opposed to the sensible heat ($L/C = 300$ K). In the calculations (see Fig. 7(a)), the effect of superheat on the growth of the columnar and equiaxed grains is significant only at high rates of heat extraction and in large castings because only under these circumstances can an appreciable temperature difference be maintained between the edge and centre of a casting. At low cooling rates and in small castings, the temperature gradient is shallow and the growth of the grains is unaffected by the initial pouring temperature. In practice, however, the effect of superheat can be dramatic, especially in small castings [19,20]. From the model, therefore, it appears not to be possible to explain satisfactorily the influence of superheat in terms of the growth of the grains: it is suggested that, as is usually proposed, the variation with superheat of the equiaxed zone and grain size is due to the delay in the bulk becoming undercooled affecting the survival of chill nuclei (the Big Bang mechanism [20]).

When a temperature dependent nucleation rate is included, the onset of equiaxed growth is delayed until the critical nucleation undercooling is attained locally causing larger equiaxed ranges and smaller equiaxed zones. If the columnar front does not exceed the critical nucleation undercooling then neither does the bulk, and no equiaxed grains are nucleated. Hence, under certain circumstances, the columnar range can be dramatically decreased by increasing the cooling rate: at a low cooling rate the columnar front might never attain the critical nucleation undercooling but on increasing the cooling rate, the front undercooling will increase and may exceed the critical value and thus permit nucleation in the bulk. It is suggested that the model could be used to investigate the efficiency of a grain refiner, thus extending the work of Maxwell and Hellawell [21].

Rapid solidification was modelled: two high values for the heat transfer coefficient ($h = 10^4$ and 10^5 W m^{-2} K^{-1}) and a thin width of casting (100 microns) were used. Nucleation undercoolings of 50 and 100 K were assumed (see Fig. 8). Rapid recalescence and a corresponding decrease in the columnar front velocity were noted. Shortly after nucleation of solid at the edge, the liquid ahead of the front is at a lower temperature and thus latent heat is conducted both into the solid and also the liquid; after the liquid has

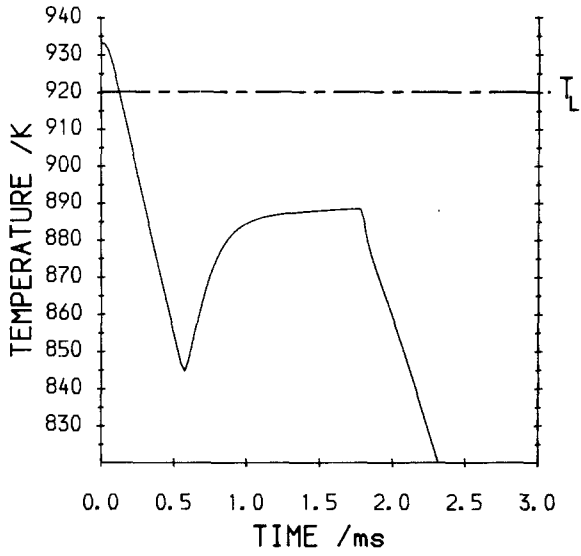

Fig. 8. Cooling curve for the rapid columnar solidification of Al-5 wt% Cu alloy. 100 um wide ribbon initially at 973 K. $h = 10^5$ Wm^{-2} K^{-1}.

recalesced, though, heat is extracted through the solid only and the front velocity falls.

Conclusions

A model for the solidification of a casting has been presented in which the columnar mass is represented as a mushy zone truncated at an undercooling which is free to vary. Equiaxed grains can exist and grow ahead of the front. Because of the freely varying undercooling and the presence of grains in the bulk, it is not possible to prescribe an enthalpy function and treat the solidification as in the usual integral, control volume enthalpy-based method. The front has to be tracked directly. Because of the truncation of the Scheil shape at the columnar tips, there is a discontinuity in the evolution of the latent heat at the columnar front: this introduces the Stefan 'jump' condition into the problem. This condition is not present in normal mushy zone models because of the continuous form assumed for the variation of bulk solid fraction with temperature. The current model, therefore, is original in so far as it is a combination of the Stefan and mushy zone models.

The model can produce realistic cooling curves and has been used to investigate the growth of equiaxed grains and the development of the equiaxed zone ahead of a columnar front. The expected trends with superheat, composition, convection and cooling rate have been reproduced. However, the superheat effect is not as pronounced in the model as that seen in practice. This is attributed to the failure of the model to consider the Big Bang mechanism for

the production of chill nuclei. The model predicts small columnar ranges and this is probably due to its neglect of the buoyancy and convective motion of the equiaxed growth ahead of the front.

Although the model requires further development to include the effects of movement of equiaxed grains, it forms a useful basis for the investigation of the evolution of the macrostructure of a casting and the interplay of the various casting parameters.

Acknowledgements

The Authors should like to thank Professor Sir Peter Hirsch FRS and the Oxford University Computing Service for the provision of office and computing facilities respectively, and one of them (SCF) is also grateful to the Royal Society of London, the United Kingdom Science and Engineering Research Council, and Alcan International Ltd for financial support.

References

1. J. Stefan: *Ann. Phys. u. Chem.* (ed. by Wiedemann) N.F., 42 (1891) 269–281.
2. N. Shamsundar: In: *Moving Boundary Problems*, ed. by D.G. Wilson, A.D. Solomon and P.T. Buggs (1981) 165–185. Pubd by Academic Press Inc., New York, U.S.A.
3. P.N. Hansen: In: *Solidification and Casting of Metals* (1979) 350–356. Pubd by Metals Society, London, U.K.
4. R.E. Marrone, J.O. Wilkes and R.D. Pehlke: *Cast Metals Research J.* 9 (1970) 184.
5. S.C. Flood and J.D. Hunt: In: *Proc. Conf. on Modeling of Casting and Welding Processes*, Henniker, New Hampshire, U.S.A. (1983) 207–218.
6. S.C. Flood: D. Phil Thesis, University of Oxford (1985).
7. T.W. Clyne: In: *Proc. 2nd Intern. Conf. on Numerical Methods in Thermal Problems*, Venice, Italy (1981) 240–256.
8. T.W. Clyne: *Metallurgical Transactions* 15B (1984) 369–381.
9. M.H. Burden and J.D. Hunt: *J. Crystal Growth* 22 (1974) Part I: 99–108, Part II: 109–116.
10. M. Tassa and J.D. Hunt: *J. Crystal Growth* 34 (1976) 38–48.
11. I. Jin and J.G. Sutherland: In: *Solidification and Casting of Metals* (1979) 256–259. Pubd by Metals Society, London, U.K.
12. R. Elliot: In: *Eutectic Solidification Processing* (1983) 247–251. Pubd by Butterworths & Co., London, U.K.
13. T.W. Clyne and W. Kurz: *Metallurgical Transactions* 12A (1981) 965–971.
14. J.D. Hunt: In: *Solidification and Casting of Metals* (1979) 3–9. Pubd by Metals Society, London, U.K.
15. J.W. Christian: In: *The Theory of Transformations in Metals and Alloys*. Part I (1975) 17–18. Pubd by Pergamon Press, Oxford, U.K.
16. J.W. Christian: ibid., 450.
17. J.D. Hunt: *Mat. Sci. Eng.* 65 (1984) 75–83.
18. B. Carnahan, H.A. Luther and J.O. Wilkes: In: *Applied Numerical Methods* (1969) 449–450. Pubd by John Wiley, New York, U.S.A.
19. B. Chalmers: In: *Principles of Solidification* (1964) 257–259, 265–268. Pubd by John Wiley, New York, U.S.A.
20. R. Morando, H. Biloni, G.S. Cole and G.F. Bolling: *Metallurgical Transactions* 1 (1970) 1407–1412.
21. I. Maxwell and A. Hellawell: *Acta Metallurgica* 23 (1975) 901–909.